microbial biotechnology

Open Access

Rapid production of L-DOPA by *Vibrio natriegens*, an emerging next-generation whole-cell catalysis chassis

Xing Liu, Xiao Han, Yuan Peng, Chunlin Tan, Jing Wang, Hongsong Xue, Ping Xu and Fei Tao*

State Key Laboratory of Microbial Metabolism, Joint International Research Laboratory of Metabolic and Developmental Sciences, School of Life Sciences and Biotechnology, Shanghai Jiao Tong University, Shanghai, China.

Summary

3, 4-Dihydroxyphenyl-L-alanine (L-DOPA) is a compound of high medical value and is considered effective as a treatment for Parkinson's disease. Currently, bioproduction of L-DOPA is mainly carried out by whole-cell catalysis mediated by recombinant *Escherichia coli* carrying heterogeneous tyrosine phenol lyase. *Vibrio natriegens* is increasingly attracting attention owing to its superiority, including extremely rapid growth and high soluble protein expression capacity. In this study, we attempt to develop an efficient whole-cell catalyst for L-DOPA production using *V. natriegens* as the chassis. The maximum soluble protein expression by *V. natriegens* was accomplished in 4 h at 37°C, which was equivalent to that achieved by *E. coli* in 16 h at 16°C. Furthermore, the maximum productivity reached over 10.0 g l^{-1} h^{-1} in the early stage of biocatalysis, nearly two-fold higher than previously reported. Approximately 54.0 g l^{-1} L-DOPA was obtained with a catechol conversion rate greater than 95%. In conclusion, *V. natriegens* displays advantages, including rapid protein expression and catalytic rate in the catalysis process for L-DOPA production. These findings strongly suggest that *V. natriegens* has remarkable potential as a whole-cell catalysis chassis for the production of valuable chemicals.

Received 13 October, 2021; accepted 26 December, 2021.
*For correspondence. E-mail taofei@sjtu.edu.cn; Tel. +86 21 34206647; Fax +86 21 34206647.
Microbial Biotechnology (2022) **15**(5), 1610–1621
doi:10.1111/1751-7915.14001
Funding information
This study was supported by the grant of the National Key R&D Program of China (2017YFC1600100).

Introduction

3, 4-Dihydroxyphenyl-L-alanine (L-DOPA) is an amino acid analog from L-tyrosine that can be used to treat Parkinson's disease (PD). During the 1960s, researchers began to utilize L-DOPA as a treatment for PD (Nagatsua and Sawadab, 2009). As a precursor of dopamine, L-DOPA can pass through the blood brain barrier and be converted into dopamine by aromatic L-amino acid decarboxylase, enabling its therapeutic use for PD treatment (Katayama and Kumagai, 2010; Min *et al*., 2013). To date, L-DOPA has been known as one of the most effective drugs for the treatment of PD. With a rising incidence and prevalence of this disease, L-DOPA has attracted remarkable attention, leading to its required quantity increasing over the years (Dorsey *et al*., 2018; Collaborators, 2019). Accordingly, global market demand of L-DOPA is approximately 250 tons per year and the total market volume has reached approximately 101 billion (Koyanagi *et al*., 2005; Min *et al*., 2015).

In the past, L-DOPA was mainly produced via extraction from plants and chemical synthesis (Chattopadhyay *et al*., 1994; Valdes *et al*., 2004). However, severe environmental pollution, time-consuming process, poor conversion rate, and low yield markedly limit their applications (Sayyed and Sudalai, 2004; Valdes *et al*., 2004; Zheng *et al*., 2018). Currently, biotechnological approaches for the production of L-DOPA, especially whole-cell catalysis, are considered efficient with advantages such as low cost, convenient operation, and high catalytic efficiency (Das *et al*., 2018; Zheng *et al*., 2018; Han *et al*., 2020). Several enzymes have been discovered and applied in whole-cell catalysis for the production of L-DOPA, among which tyrosine phenol lyase (TPL) is relatively well elucidated (Lee and Xun, 1998; Krishnaveni *et al*., 2009; Min *et al*., 2015). TPL (E.C.4.1.99.2) is an enzyme that can reversibly catalyze the β-elimination of L-tyrosine to generate pyruvate, phenol and ammonia, depending on pyridoxal 5′-phosphate (PLP) as a coenzyme (Milic *et al*., 2011). L-DOPA can be synthesized in one step by TPL if the substrate phenol is substituted by catechol. The TPL-mediated method for L-DOPA production displays good performances and overcomes major shortcomings of other enzymes, ultimately stimulating comprehensive researches on different TPLs. TPLs isolated from *Fusobacterium nucleatum* (Zheng *et al*., 2018), *Erwinia herbicola* (Zeng *et al*.,

2019), *Citrobacter freundii* (Chandel and Azmi, 2013), and other microorganisms have been utilized for L-DOPA production (Yuan *et al*., 2020; Zhu *et al*., 2020).

Currently, *E. coli* is regarded as the primary microbial chassis of whole-cell catalysis for L-DOPA production. However, existing technology cannot meet the current growing demand, although the potential of *E. coli* cell has been extensively explored following decades of development. *Vibrio natriegens* is a nonpathogenic gram-negative marine bacterium first discovered in 1958. With a doubling time less than 10 min, this bacterium is known to be the fastest growing microorganism to date, and is two-fold faster than *E. coli* (Eagon, 1962). *V. natriegens* also possesses a wide substrate spectrum and could survive on a variety of carbon resources with high substrate uptake rates (Hoffart *et al*., 2017). *V. natriegens* equipped with the T7 expression system has a preferable soluble protein expression capacity (Weinstock *et al*., 2016). Abundant ribosomes in *V. natriegens* contribute to its capabilities of high-level and rapid protein expression (Hoff *et al*., 2020). Moreover, accurate control of induction timing is unnecessary because the protein expression level is impervious to biomass concentration of the induction timing, which is effortless and time-saving (Becker *et al*., 2019). *V. natriegens* may also highly express some genes, acting as an expression host superior to *E. coli* in some aspects (Xu *et al*., 2021). Based on the above findings, it is reasonable to speculate that *V. natriegens* is a promising novel whole-cell catalysis chassis for L-DOPA production.

In this study, we attempted to employ *V. natriegens* to produce L-DOPA through whole-cell catalysis. First, we compared several TPLs from different sources and selected the TPL from *F. nucleatum* (FnTPL) as a target based on its high catalytic activity. Thereafter, we introduced the vector pET-28(a) harboring target gene *tpl* into *V. natriegens*. After the assessment of protein expression and condition optimization, fed-batch experiments were carried out to produce L-DOPA through whole-cell catalysis. Eventually, approximately 54.0 g l^{-1} L-DOPA was obtained in 10 h, with productivity being greater than 10.0 g l^{-1} h^{-1} in the early stage, which was higher than that reported for *E. coli*. Overall, our findings provide persuasive evidence that *V. natriegens* may be capable of becoming a novel whole-cell catalysis chassis.

Results

Construction of recombinant V. natriegens *and* E. coli

Vmax is a genetically engineered strain derived from *V. natriegens* ATCC14048 by integrating the T7 RNA polymerase expression cassette at the *dns* locus. Vmax is a commercially available and pET-compatible strain with efficient transformation and strong protein expression ability. Accordingly, Vmax was selected as target strain while *E. coli* BL21 (DE3) was used as a control. The recombinant vector pET-28a(+)-FnTPL (vector pET-28a (+) harboring gene *tpl* from *F. nucleatum*) was introduced into these two strains. The obtained recombinant strain Vmax-1 (Vmax-pET-28a(+)-FnTPL) and recombinant strain BL21-1 (*E. coli* BL21 (DE3)-pET-28a(+)-FnTPL) were used for the subsequent experiments. Bacterial strains used in this study are summarized in Table S1.

Investigation of TPL expression and catalytic function

After the construction of recombinant strains, protein expression and catalytic function were assessed. First of all, in terms of biocatalyst production, only 1.5 h was required to reach an OD_{600} of approximately 0.6 for *V. natriegens,* which was two-fold shorter than that of *E. coli*, highlighting its remarkable advantage in growth rate. Then, based on the single band obtained via SDS-PAGE, the molecular weight of protein FnTPL is determined to be approximately 52 kDa, which is consistent with the calculated value (Fig. 1A). Most target proteins formed inclusion bodies in BL21-1 induced at 37°C. Soluble protein expression was achieved both in Vmax-1 induced at 37°C for 4 h and BL21-1 induced at 16°C for 16 h. Besides, their soluble expression bands were almost equivalent, indicating that *V. natriegens* was capable of solubly expressing the protein, FnTPL, at a rapid rate.

To verify whether the target protein possessed catalytic function, whole-cell catalysis for L-DOPA production was performed using these two recombinant strains. Based on the catalytic results, both Vmax-1 and BL21-1 can produce L-DOPA. The titer of L-DOPA produced by Vmax-1 was three-fold higher than that of BL21-1 under the same circumstances (Fig. 1B). The high catalytic rates obtained herein initially suggest that Vmax-1 is a suitable whole-cell catalysis chassis.

Optimization of the induction time for protein expression

Induction time is an important factor influencing protein expression. IPTG inductions of protein expression by Vmax-1 were performed at 37°C with durations ranging from 0 h to 6 h. The maximum protein expression was defined as 100% relative protein expression. According to the results (Fig. 1C), protein expression level reached a peak with induction for 4 h while soluble protein expression level decreased and formed inclusion bodies with an extended period of induction (Fig. S1). Besides, OD_{600} basically remained constant after 4 h, indicating that cells entered into stationary phase. More importantly, the catalytic activity of whole-cell over induction

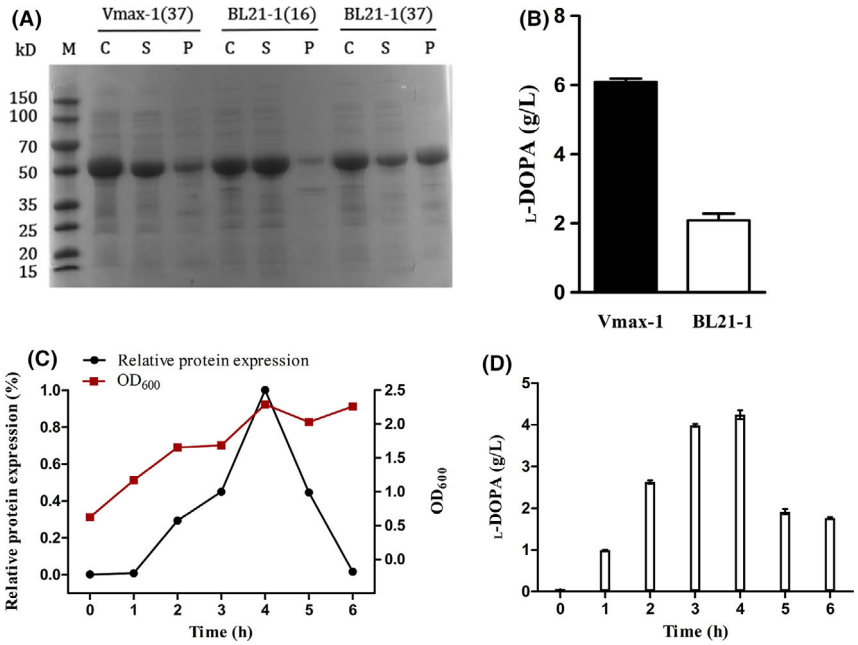

Fig. 1. Investigation and optimization of soluble protein expression and verification of catalytic function.
A. Comparison of protein expression between Vmax-1 and BL21-1 under different induction conditions. M, marker; C, cell lysates; S, supernatants; P, precipitates; Vmax-1(37), Vmax-1 induced at 37°C; BL21-1(16), BL21-1 induced at 16°C; BL21-1(37), BL21-1 induced at 37°C.
B. Verification of catalytic function.
C. Optimization of induction time for maximum soluble protein expression.
D. Catalytic activity of whole-cell over induction time. Black circle represented relative protein expression, red square represented OD_{600}. Error bars represented the SD of $n = 3$ biological replicates.

time was also investigated (Fig. 1D). The catalytic activity reached the maximum at 4 h, thereby aligning with the level of soluble protein expression. Taken together, these results reinforce the fact that being induced 4 h at 37°C was the optimal condition for protein expression of TPL by Vmax-1. Therefore, protein expression by Vmax-1 induced for 4 h at 37°C was applied in the subsequent experiments.

In terms of BL21-1, the protein expression at 16°C was also optimized. The level of soluble protein expression increased, reaching its peak at 16 h. However, protein expression level began to decline with extended induction (Fig. S2). Consequently, protein expression by BL21-1 induced for 16 h at 16°C was considered optimal and was employed in the subsequent experiments.

Optimization of the initial concentration of substrates for L-DOPA production

The concentrations of substrates had a great impact on TPL-mediated L-DOPA production. The accumulation of catechol will exert toxicity to cells and irreversible inhibitory effect on TPL. Further, excessive pyruvate sodium will initiate a nonenzymatic reaction with L-DOPA to form by-products, which are harmful to the whole process (Enei *et al*., 1973). As a result, proper concentration of substrates plays an important role in enhancing the titer of L-DOPA. To investigate the optimal initial concentration, the concentrations of two substrates were fixed and the concentration of the other substrate was changed in gradient in the reaction mixtures. The titer of L-DOPA was found to reach a peak when the concentration of catechol attained 7.5 g l^{-1}. Further, there was an evident decrease in titers with a further increase in concentrations (Fig. 2A), which probably resulted from the deactivation of the enzyme caused by excessive catechol. In terms of ammonium acetate, the titer of L-DOPA reached the highest level when the concentration was fixed at 50.0 g l^{-1} and the catalytic activities also decreased with higher concentration (Fig. 2C). With regard to sodium pyruvate, the titer of L-DOPA increased slowly as the concentration of sodium pyruvate increased (Fig. 2B). Excessive sodium pyruvate would not only enhance the conversion rate of catechol but also react with L-DOPA to produce harmful byproducts leading to reduction of L-DOPA titer in the subsequent fed-batch experiments, and 10.0 g l^{-1} sodium pyruvate was selected as the optimal concentration. The optimal concentration of catechol for *V. natriegens* was higher than that reported for *E. coli*, indicating stronger tolerance to catechol for *V. natriegens*. No obvious difference was identified in the other two substrates between these

two strains (Tang *et al*., 2018). Altogether, 7.5 g l^{-1} catechol, 10.0 g l^{-1} sodium pyruvate, and 50.0 g l^{-1} ammonium acetate were selected as the optimal initial concentrations for the next experiments.

Optimization of the temperature and pH for L-DOPA production

Temperature and pH are essential factors in enzymatic reactions. To determine the optimal temperature and pH, whole-cell catalysis was carried out at different temperatures and pHs with other conditions remaining the same. The optimal temperature was investigated at four common temperatures: 20°C, 30°C, 37°C, and 50°C. The maximum titer of L-DOPA was obtained at 37°C, which was higher than that of 20°C and 30°C (Fig. 2D). L-DOPA titer decreased at 50°C that was presumably caused by the instability of L-DOPA at higher temperatures. This result was different compared to a previous study, in which the maximum titer of L-DOPA was acquired at 30°C for *E. coli* (Tang *et al*., 2018).

In terms of stability of the whole cell at different temperatures, the initial catalytic activities at 37°C were defined as 100% relative activity. The stability of the whole cell deteriorated as temperature increased (Fig. 2E). Moreover, the catalytic activity markedly decreased at 50°C with only 50% of its initial catalytic activity remaining in 6 h. The situation was similar at both 30°C and 37°C as the catalytic activities decreased to approximately 60% of the maximum catalytic activity in 16 h. The whole cell was extremely stable at 20°C with more than 90% of initial catalytic activity remaining in 24 h.

On account of the instability of L-DOPA, the liability of condensation of L-DOPA with pyruvate, extra by-product formation at high temperature (Tang *et al*., 2018), and better stability of whole-cell under low temperature, 20°C was selected as the optimal temperature for the further fed-batch experiments in order to achieve higher titer of L-DOPA with fewer by-products formation.

The optimal pH was investigated in reaction mixtures with pH ranging from 4.0 to 10.5. As shown in Fig. 2F, the maximum catalytic activity was obtained in phosphate buffer (potassium phosphate buffer, pH 8.0), which was consistent with previous research (Tang *et al*., 2018). However, in Tris-HCl buffer (pH 8.0), it appeared with a lower catalytic activity. It was reported that potassium ion can promote the activity of TPL and bind to TPL to improve the affinity of TPL to PLP (Kumagai *et al*., 1970; Demidkina *et al*., 2009). This may partially explain the lower catalytic activity in Tris-HCl buffer (pH 8.0) than phosphate buffer (pH 8.0). The catalytic activities were absolutely lost when the pH was too low (pH < 6.0) or too high (pH > 10.5). Therefore, the reactions were conducted in phosphate buffer (pH 8.0) for the subsequent experiments.

Time course of the whole-cell catalysis process

Prior to the fed-batch whole-cell catalysis experiments, it was necessary to figure out the feeding strategy of substrates to prevent the inactivation of TPL caused by an accumulation of catechol. Time-course experiments were carried out in the optimal conditions determined above. Catechol was almost consumed and the reaction reached equilibrium in 1 h (Fig. 3A). The titer of L-DOPA remained unchanged thereafter. The catalytic rate during the first half-hour was higher than the following half-hour, which was mainly due to substrate depletion. According to the results, a feeding strategy of a supplement of 7 g l^{-1} of catechol, 7 g l^{-1} of sodium pyruvate and 5.6 g l^{-1} of ammonium acetate per hour in the early stage were determined. Subsequently, the feeding strategy was adjusted by feeding 3.5 g l^{-1} of catechol, 3.5 g l^{-1} of sodium pyruvate, and 2.8 g l^{-1} of ammonium acetate per hour owing to the inevitable decline of catalytic rates in the later stage of the whole-cell catalysis.

Biosynthesis of L-DOPA via a two-stage fed-batch strategy

Following optimization, biosynthesis of L-DOPA through whole-cell catalysis by Vmax-1 was carried out in a stirred 1-l bioreactor by adopting a two-stage fed-batch strategy. Sodium sulfite was added to the reaction mixture to protect oxygen-sensitive catechol and L-DOPA from being oxidized. Ethylenediaminetetraacetic acid was used to minimize the possibility of the nonenzyme reaction between L-DOPA and pyruvate as well as to maintain enzymatic activity as a metal chelating agent (Katayama and Kumagai, 2010; Tang *et al*., 2018). To maintain substrates at optimal concentrations, 7.0 g l^{-1} of catechol, 7.0 g l^{-1} of sodium pyruvate, and 5.6 g l^{-1} of ammonium acetate were supplied per hour in the first 4 h. With the reaction proceeding and catalytic rate decreasing, a supplement of 3.5 g l^{-1} of catechol, 3.5 g l^{-1} of sodium pyruvate, and 2.8 g l^{-1} of ammonium acetate per hour was adopted to avoid the accumulation of substrates. The whole catalytic process by Vmax-1 was shown in Fig. 3B. Owing to the fast catalytic rate in the first 4 h, approximately 40.0 g l^{-1} of L-DOPA was produced with a productivity of approximately 10.0 g l^{-1} h^{-1}, which was nearly two-fold higher than that obtained by *E. coli* (Tang *et al*., 2018). However, the catalytic activities decreased in the subsequent process. Eventually, the titer of L-DOPA was approximately 54.0 g l^{-1} in 10 h with average productivity over 5.0 g l^{-1} h^{-1} and conversion rate of catechol over 95%,

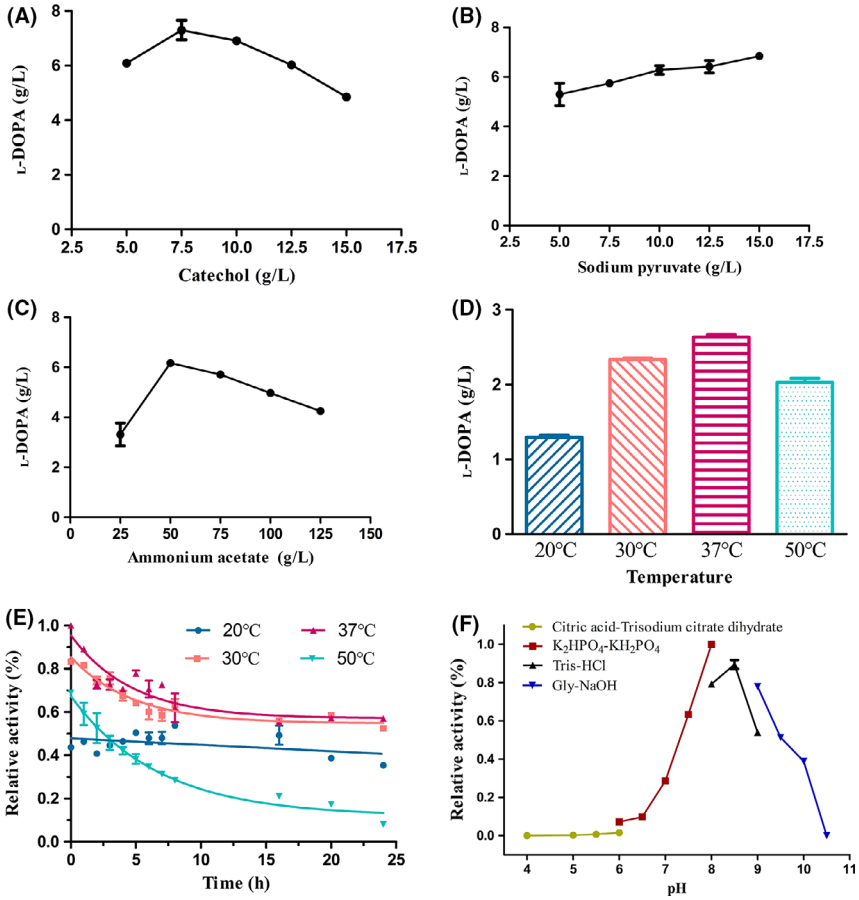

Fig. 2. Optimization of different parameters of catalysis system.
A. Optimization of initial concentration of catechol.
B. Optimization of initial concentration of sodium pyruvate.
C. Optimization of initial concentration of ammonium acetate.
D. The effect of different temperatures on catalytic activity.
E. Stability of whole-cell at different temperatures. Blue circle represented 20°C, orange square represented 30°C, garnet triangle represented 37°C, cyan inverted triangle represented 50°C.
F. The effect of different pHs on catalytic activity. Tawny circle represented citric acid-trisodium citrate dehydrate buffer (4.0–6.0), red square represented phosphate buffer (6.0–8.0), black triangle represented Tris-HCl buffer (8.0–9.0), blue inverted triangle represented Gly-NaOH buffer (9.0–10.5). Error bars represent the SD of $n = 3$ biological replicates.

which is comparable with that of *E. coli* using the same TPL (Zheng *et al*., 2018). With the further addition of substrates, catechol was no longer consumed and gradually accumulated.

It is noted that the enzymatic activities declined during the process, which might be partially attributed to bacterial autoaggregation according to the evidence that cells clumped and aggregated at the bottom of the reactor (Fig. S3). Therefore, we attempted to knock out some key genes in the metabolic pathway of exopolysaccharides in *V. natriegens* to inhibit bacterial autoaggregation. Given its close relationship to *Vibrio cholerae*, we selected the geneencoding undecaprenyl-phosphate glucose phosphotransferase (PN96_RS15190) analogous to gene *vpsO* in *Vibrio cholerae* as a target gene. Gene *vpsO* was reported to be important in exopolysaccharide production and biofilm formation (Fong *et al*., 2010; Schwechheimer *et al*., 2020). Then, a mutant strain Vmax-2 was obtained and hired to conduct whole-cell catalysis for L-DOPA production. However, only approximately 47.0 g l^{-1} of L-DOPA was produced in 10 h using this mutant strain and the titer of L-DOPA no longer increased as found for the wild-type strain (Fig. 3C). In consequence, more efforts are required to solve this problem.

For further verification and comparison, biosynthesis of L-DOPA through whole-cell catalysis mediated by recombinant strain BL21-1 was carried out (Fig. 3D). Approximately 34.0 g l^{-1} of L-DOPA was produced in 9 h with average productivity of approximately 3.8 g l^{-1} h^{-1}. According to the results, the fed-batch catalysis process was quite similar to that of Vmax-1 and Vmax-2. Based on these facts, the *V. natriegens*

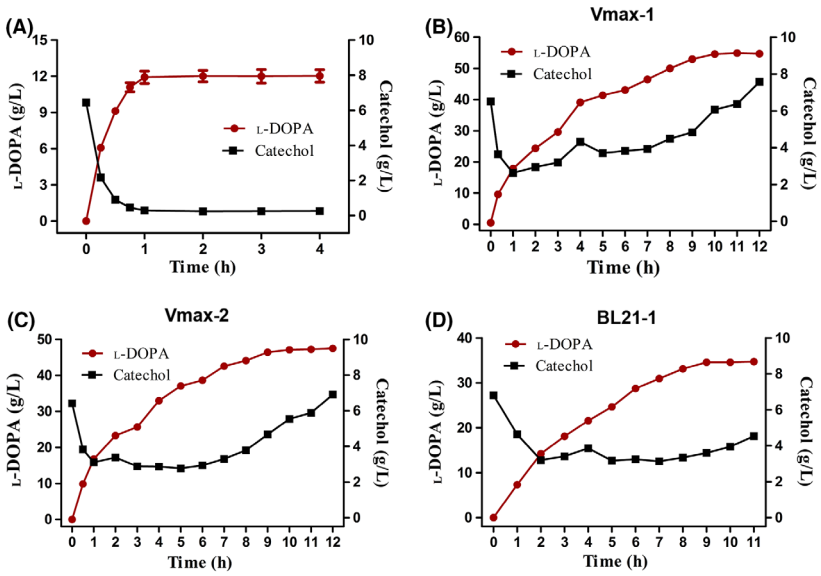

Fig. 3. Biosynthesis of L-DOPA by recombinant strain through whole-cell catalysis.
A. Time course of whole-cell catalysis by Vmax-1 without feeding.
B. Biosynthesis of L-DOPA by resting cells of Vmax-1 with a two-stage fed-batch strategy.
C. Biosynthesis of L-DOPA by resting cells of Vmax-2 with a two-stage fed-batch strategy.
D. Biosynthesis of L-DOPA by resting cells of BL21-1 with a two-stage fed-batch strategy. Red circle represented concentration of L-DOPA, black square represented concentration of catechol. Error bars represented the SD of $n = 3$ biological replicates.

system seemed superior to the *E. coli* system in the aspects of titer and productivity under the same conditions. Nonetheless, more efforts are needed to improve the titer of L-DOPA produced by *V. natriegens*.

Discussion

Microbial chassis plays a vital role in the whole-cell catalysis process as production efficiency, cost, and stability of biocatalysts are determined by microbial chassis (Lin and Tao, 2017). *E. coli* is the most commonly used chassis microorganism due to its clear genetic background and convenient genetic manipulation. In fact, *E. coli* has been applied in L-DOPA production for many years, and several achievements in L-DOPA production have been made with this traditional strain. However, there are limitations to its industrial application, such as time-consuming, costly, and risky of being contaminated, which are necessary to be overcome. *V. natriegens* appears superior to be microbial chassis as an alternative to *E. coli* due to its rapid growth rate and capability of protein expression (Weinstock *et al*., 2016; Becker *et al*., 2019). Studies involving *V. natriegens* mainly focused on genome organization, synthetic biology, and metabolic engineering (Becker *et al*., 2019; Tschirhart *et al*., 2019; Zhang *et al*., 2021). However, whole-cell catalysis approaches using *V. natriegens* have rarely been reported. In the present study, L-DOPA was selected as the target compound to verify the productive potential of *V. natriegens* in whole-cell catalysis. As expected, L-DOPA production by *V. natriegens* was accomplished successfully in this study. In order to better demonstrate the advantages of this novel host, a summary of the comparison of various TPLs from different sources for L-DOPA production is given in Table 1. Expressing TPL in *V. natriegens* showed preferable superiorities in several aspects. In terms of biocatalyst production, only 1.5 h was required to reach an OD_{600} of approximately 0.6 for *V. natriegens*, which is two-fold shorter than that of *E. coli*. The maximum soluble protein expression of *V. natriegens* was acquired at 37°C for 4 h, whereas 16 h at 16°C was required by *E. coli* to achieve the same level of soluble protein expression. Cell culture and protein expression of *V. natriegens* could be performed at the same temperature, bypassing adjustment of temperatures, which is favorable for industrial applications. The characteristics of rapid growth rate and protein expression shortened the time and simplified the process, rendering Vmax-1 an ideal host for TPL expression and L-DOPA production. Thus, the use of *V. natriegens* as a host for L-DOPA production could curtail the production cycle, and reduce labor and costs, especially when applied on a larger scale, suggesting its great economical potential. A final concentration of 54.0 g l^{-1} of L-DOPA was obtained in 10 h with maximum productivity over 10.0 g l^{-1} h^{-1} in the early stages and overall productivity of approximately 5.4 g l^{-1} h^{-1}. The overall productivity was higher than that reported for *E. coli*. Moreover, better

Table 1. Comparison of different tyrosine phenol lyases for L-DOPA production through whole-cell catalysis.

Strain (enzyme)	Cell culture time (h)	Induction time (temperature) (h °C^{-1})	Titer (g l^{-1})	Productivity (g l^{-1} h^{-1})	Refs.
V. natriegens (*Fn*-TPL)	~ 1.5	4/37	54.3	5.4	This study
E. coli (*Fn*-TPL)	~ 3	16/16	34.8	3.5	This study
E. coli (*Eh*-TPL)	–	8/25	69.1	11.5	Zeng *et al.* (2019)
E. coli (*Ki*-TPL)	–	10/25	114.8	7.2	Yuan *et al.* (2020)
E. coli (*Ss*-TPL)	–	–	29.8	5.0	Lee *et al.* (1996)
E. coli (*Fn*-TPL)	–	10/20–28	121.5	4.9	Tang *et al.* (2018)
E. coli (*Cf*-TPL)		–	2.8	0.3	Park *et al.* (1998)

Fn-/*Eh*/*Ki*-/*Ss*-/*Cf*-TPL means that the TPL originated from *Fusobacterium nucleatum*, *Erwinia herbicola*, *Kluyvera intermedia*, *Symbiobacterium* sp., and *Citrobacter freundii*, respectively.

performances in the aspects of titer and productivity were achieved by Vmax-1 compared to BL21-1 under the same conditions in our laboratory, indicating that *V. natriegens* may have remarkable potential for serving as a whole-cell catalysis chassis for L-DOPA production. In summary, featured with rapid protein expression and catalytic rate, *V. natriegens* is considered promising for future application and serves as an efficient whole-cell biocatalyst for other valuable chemicals.

As described above, *V. natriegens* shows a rapid catalytic rate during the biocatalysis process, with maximum productivity nearly twice as high as that obtained with *E. coli*. In fact, *V. natriegens* has the highest catalytic rate reported to date for this TPL from *F. nucleatum*. Its good performance reflects its underlying application value in whole-cell catalysis, which makes it necessary to explore the underlying mechanism. The mean cell volume of *V. natriegens* in the stationary phase is estimated to be 0.93 μm^3 cell^{-1}, which indicates that it possesses a large specific surface area (Fagerbakke *et al.*, 1996). This will increase the contact area with substrates, facilitate the transportation of substances, and further promote catalytic activities of whole-cell catalysis, which is consistent with the high catalytic rate obtained in this study. Therefore, various compounds, especially those with mass transfer resistance, could be promisingly produced by *V. natriegens*.

Enzymatic activities were found to decline during the process (Fig. 3B). According to a previous research, L-DOPA is slightly soluble in water and precipitates when its concentration exceeds 10.0 g l^{-1} (Tang *et al.*, 2018). Thereafter, the small precipitated particles tend to attach to the cell surfaces and wrap the cells. As a result, it would severely hinder the substrates from entering the cells. This phenomenon has been reported for recombinant *E. coli* cells during the process of L-DOPA production (Tang *et al.*, 2018). White precipitated particles were identified during the process using recombinant *V. natriegens*. Therefore, we speculate that a similar phenomenon might occur during the process, thereby exerting an indirect negative influence on the catalytic activity of biocatalysis. In addition, bacterial autoaggregation is a widespread phenomenon existing in various environmental and pathogenic bacteria. It may be induced by the stressful and poor environmental conditions to protect against external stresses mediated by agglutinin such as exopolysaccharides (Trunk *et al.*, 2018). Bacterial autoaggregation of *V. natriegens* was presumed to occur during the process, which could be demonstrated by cell clumping and aggregation at the bottom of the reactor (Fig. S3). This behavior of bacterial autoaggregation might act as a physical barrier to block substrates and affect catalysis. However, we fail to inhibit bacterial autoaggregation by gene knockout, and only approximately 47.0 g l^{-1} of L-DOPA was produced in 10 h, which was lower than that achieved with the wild-type strain. Cell clumps were identified after biocatalysis, suggesting that this gene knockout failed to inhibit bacterial autoaggregation. Consequently, systematic and combinatorial gene knockouts are required to perform in the metabolic pathway of exopolysaccharides in *V. natriegens* in subsequent studies. Owing to these modifications, *V. natriegens* may become a promising candidate for the development of an efficient and stable whole-cell catalysis platform.

In conclusion, bioproduction of L-DOPA was carried out by *V. natriegens* in this study. *V. natriegens* displayed remarkable growth rate and protein expression capacity, and has a rapid catalytic rate in whole-cell catalysis. This study highlights its remarkable competence to act as a novel whole-cell catalysis chassis for the production of L-DOPA.

Experimental procedures

Chemicals

L-DOPA standard and pyruvate sodium were purchased from Aladdin BioChem Technology (Shanghai, China). Catechol, ammonium acetate, sodium sulfite, and

ethylenediamine tetraacetic acid disodium salt were purchased from Sinopharm Chemical Reagent (Shanghai, China). The cozyme pyridoxal 5′-phosphate (PLP) was purchased from Bide Pharmatech (Shanghai, China). Medium components such as tryptone and yeast extract were purchased Oxoid (Basingstoke, England). Antibiotic kanamycin and isopropyl 1-β-D-thiogalactopyranoside (IPTG) were bought from Sangon Biotech (Shanghai, China). All other chemicals were analytic grade and purchased from commercial sources.

Construction of recombinant V. natriegens *and* E. coli

The DNA sequences of TPL from *F. nucleatum* were acquired from NCBI database. The target gene with codon optimized against *V. natriegens* was synthesized by Genewiz Biotech (Suzhou, China). The synthesized gene was flanked with two endonuclease restriction sites *Nco*I and *Xho*I. The gene segment was digested by *Nco*I and *Xho*I (New England Biolabs) at 37°C in a water bath. Then it was ligated with the linearized plasmid pET-28a (+) digested by the same restriction endonuclease at 16°C overnight in order to obtain recombinant plasmid pET-28a(+)-FnTPL. Vmax Express (Synthetic Genomics, La Jolla, California, USA) was a commercially available *V. natriegens* type, which was derived from *V. natriegens* ATCC14048 by integrating the T7 RNA polymerase expression cassette at the *dns* locus. The derived plasmid pET-28a(+)-FnTPL was transformed into Vmax through electroporation. First, mix 10–100 ng of plasmid and electroporation-competent cells of Vmax Express in the cuvettes. Then set up the electrotransformation program (1400–1800 V, 200 Ω, and 2 mm) and perform electrotransformation. Next, add 1 ml of LBv2 medium (consisting of 5 g l^{-1} of yeast extract, 10 g l^{-1} of peptone, 30 g l^{-1} of NaCl) to resuspend the cells and transfer the suspension to a 1.5-ml centrifuge tube, and incubate the cells for 2 h at 37°C in an incubator. Finally, apply the bacterial solution onto the LBv2 agar plate with kanamycin resistance to screen out the correct recombinant strain. Similarly, the plasmid pET-28a(+)-FnTPL was also transformed into *E. coli* BL21 (DE3) through heat shock transformation. First, the plasmid was added to the competence cells of *E. coli* BL21 (DE3) and incubated on ice for 30 min, followed by heat shock for 30 s and then placed on ice for 2 min. Then, adding 1 ml of LB medium (consisting of 5 g l^{-1} of yeast extract, 10 g l^{-1} of peptone, 10 g l^{-1} of NaCl) into the 1.5-ml centrifuge tube and incubated at 37°C for 1 h. Finally, the bacterial solution was applied onto LB agar plate containing kanamycin resistance to screen out the correct recombinant strain. It was worth noting that because strain Vmax had resistance to kanamycin naturally, the concentration of kanamycin for screening recombinant Vmax was higher than the normal working concentration. Therefore, the fluid medium or solid agar plates for screening recombinant *E. coli* BL21 (DE3) were supplemented with 50 μg ml^{-1} kanamycin while 200 μg ml^{-1} kanamycin was supplemented for screening recombinant Vmax.

Characterization of soluble protein expression and catalytic function

The recombinant strain Vmax-pET-28a(+)-FnTPL, named as Vmax-1, were cultured at 37°C in LBv2 medium supplemented with 200 μg ml^{-1} kanamycin and recombinant *E. coli* BL21 (DE3)-pET-28a(+)-FnTPL, named as BL21-1, were cultured at 37°C in LB medium supplemented with 50 μg ml^{-1} of kanamycin. When optimal density at 600 nm (OD_{600}) of cultures reached around 0.6, IPTG was added into the cultures to a final concentration of 0.5 mM in order to induce protein expression for both of the recombinant strains. The induction for Vmax-1 was performed at 37°C for 4 h. As for BL21-1, the induction was performed at 37°C for 4 h or 16°C for about 16–20 h. Cells of both strains were collected by centrifugation at 4000 r.p.m. for 20 min after induction. Cell pellets were suspended and washed twice by phosphate buffer solution and suspended to an equal OD_{600} for these two strains. Then, bacterial suspension was subjected to cell disruption by a high-pressure homogenizer (Antos Nano Technology, Suzhou, China). Cell lysates were centrifuged at 10 000 *g* for 40 min to separate supernatants and precipitations. Finally, sodium dodecyl sulfate-polyacrylamide gel electrophoresis (SDS-PAGE) analysis was carried out to investigate and compare the level of the protein expression per OD_{600} of these two strains under different induction conditions.

For the verification of catalytic function, cells of both strains were collected by centrifugation at 4000 r.p.m. for 20 min after induction. Then cell pellets were washed twice by phosphate buffer solution and afterward suspended with a suitable volume of phosphate buffer solution. Cell suspensions were used for the catalytic reaction. The reaction mixture consisted of phosphate buffer solution, 5.0 g l^{-1} of catechol, 6.0 g l^{-1} of pyruvate sodium, 50.0 g l^{-1} of ammonium acetate, 2.0 g l^{-1} of sodium sulfite, 1.0 g l^{-1} of ethylenediamine tetraacetic acid disodium salt, 1 mM of PLP and resting cells of Vmax-1 or BL21-1 with a final OD_{600} of 20 in a total volume of 50 ml. The reaction mixture (pH 8.0) was carried out at 30°C with shaking at 200 r.p.m. for 1 h. Then an equal volume of 4 M HCl was added to terminate the reaction. Samples were further detected by High-Performance Liquid Chromatography (HPLC) to determine the concentration of L-DOPA. All experiments were carried out in triplicate.

Optimization of induction time for protein expression

The cells were cultured and induced as described above. The induction time was ranged from 0 h to 6 h. OD_{600} of each group before collection was determined and cells were collected by centrifugation at 4000 r.p.m. for 20 min after induction. All cell pellets were washed twice by phosphate buffer solution and afterward suspended to an equal OD_{600} with a suitable volume of phosphate buffer solution. Then, part of bacterial suspension was subjected to cell disruption by a high-pressure homogenizer. Cell lysates were centrifuged at 10 000 *g* for 40 min to separate supernatants and precipitations. SDS-PAGE analysis was carried out to compare the level of protein expression under different induction periods. Relative quantification of protein expression was accomplished by the software ImageJ. The rest of bacterial suspension was subjected to catalysis reactions to investigate the effect of induction time on whole-cell catalytic activities. All the reactions were conducted in 10 ml of reaction mixture (pH 8.0) containing phosphate buffer solution, 7.5 g l^{-1} of catechol, 10.0 g l^{-1} of pyruvate sodium, 50.0 g l^{-1} of ammonium acetate, 2.0 g l^{-1} of sodium sulfite, 1.0 g l^{-1} of ethylenediamine tetraacetic acid disodium salt, 1 mM of PLP, and resting cells of Vmax-1 with a final OD_{600} of 20. All the reactions lasted for 30 min at 30°C with shaking at 200 r.p.m. until the same volume of 4 M of HCl was added. Samples were further detected by HPLC. All experiments were carried out in triplicate.

Optimization of initial concentration of substrates on L-DOPA production

The investigation of optimal concentration of different substrates was conducted in 50 ml of reaction mixture (pH 8.0) containing phosphate buffer solution, 2.0 g l^{-1} of sodium sulfite, 1.0 g l^{-1} of ethylenediamine tetraacetic acid disodium salt, 1 mM of PLP, resting cells of Vmax-1 with a final OD_{600} of 20, and different concentrations of catechol, pyruvate sodium, or ammonium acetate at 30°C. The concentration of catechol varied from 5.0 g l^{-1} to 15.0 g l^{-1} while the concentrations of pyruvate sodium and ammonium acetate were fixed at 10.0 g l^{-1} and 50.0 g l^{-1}, respectively. Similarly, the concentration of pyruvate sodium varied from 5.0 g l^{-1} to 15.0 g l^{-1} while the concentrations of catechol and ammonium acetate were fixed at 5.0 g l^{-1} and 50.0 g l^{-1}, respectively. And with the concentrations of catechol and pyruvate sodium fixed at 5.0 g l^{-1} and 10.0 g l^{-1}, respectively, the concentration of ammonium acetate ranged from 25.0 g l^{-1} to 125.0 g l^{-1} to determine the optimal conditions. All the reactions lasted for 1 h with shaking at 200 r.p.m. until the same volume of 4 M of HCl was added. Samples were further detected by HPLC. All experiments were carried out in triplicate.

Optimization of temperature and pH on L-DOPA production

The effect of temperature on L-DOPA production was investigated in 50 ml of reaction mixture (pH 8.0) containing phosphate buffer solution, 7.5 g l^{-1} of catechol, 10.0 g l^{-1} of pyruvate sodium, 50.0 g l^{-1} of ammonium acetate, 2.0 g l^{-1} of sodium sulfite, 1.0 g l^{-1} of ethylenediamine tetraacetic acid disodium salt, 1 mM of PLP, and resting cells of Vmax-1 with a final OD_{600} of 20 at some common temperatures including 20°C, 30°C, 37°C, and 50°C. All the reactions lasted for 1 h with shaking at 200 r.p.m. until the same volume of 4 M of HCl was added. Samples were further detected by HPLC.

The effect of pH on L-DOPA production was investigated in 50 ml of reaction mixture containing buffers with different pH values, 7.5 g l^{-1} of catechol, 10.0 g l^{-1} of pyruvate sodium, 50.0 g l^{-1} of ammonium acetate, 2.0 g l^{-1} of sodium sulfite, 1.0 g l^{-1} of ethylenediamine tetraacetic acid disodium salt, 1 mM of PLP, and resting cells of Vmax-1 with a final OD_{600} of 20 at 30°C. The pH values ranged from 4.0 to 10.5 adjusted by several buffer solutions, including citric acid-trisodium citrate dehydrate buffer (4.0–6.0), phosphate buffer (6.0–8.0), Tris–HCl buffer (8.0–9.0), and Gly-NaOH buffer (9.0–10.5). All the reactions lasted for 1 h with shaking at 200 r.p.m. until the same volume of 4 M of HCl was added. Samples were further detected by HPLC. All experiments were carried out in triplicate.

Stability of whole-cell biocatalysts at different temperatures

After the cells were cultured, induced, collected, and washed as described above, cell pellets were suspended and divided into four equal parts. Then the four parts of cell suspension were incubated for 24 h at different temperatures including 20°C, 30°C, 37°C, and 50°C. Take part of the resting cells out at regular intervals for the catalytic reaction. All reaction mixtures (pH 8.0), containing phosphate buffer solution, 7.5 g l^{-1} of catechol, 10.0 g l^{-1} of pyruvate sodium, 50.0 g l^{-1} of ammonium acetate, 2.0 g l^{-1} of sodium sulfite, 1.0 g l^{-1} of ethylenediamine tetraacetic acid disodium salt, 1 mM of PLP, and resting cells of Vmax-1 with a final OD_{600} of 20, were performed at the corresponding temperatures with shaking at 200 r.p.m. for 30 min. And then an equal volume of 4 M HCl was added to terminate the reactions. All samples were further analyzed by HPLC. All experiments were carried out in triplicate.

Time course of whole-cell catalysis process

After the cells were cultured, induced, collected, and washed as described above, cell pellets were suspended for the catalytic reaction. The reaction mixture (pH 8.0) containing phosphate buffer solution, 7.5 g l^{-1} of catechol, 10.0 g l^{-1} of pyruvate sodium, 50.0 g l^{-1} of ammonium acetate, 2.0 g l^{-1} of sodium sulfite, 1.0 g l^{-1} of ethylenediamine tetraacetic acid disodium salt, 1 mM of PLP and resting cells of Vmax-1 with a final OD_{600} of 20 at 20°C and 200 r.p.m. Samples were taken every 15 min in the first 1 h and every hour thereafter until the substrate was depleted. All samples were further analyzed by HPLC. All experiments were carried out in triplicate.

Knock-out gene of Vmax derived from V. natriegens *ATCC14048*

For the deletion of PN96_RS15190, named as gene *vps*, the flanking regions 600-bp upstream and 600-bp downstream were amplified and then cloned into the *Bam*HI/*Eco*I site of plasmid pKR6K, resulting in plasmid pKR6KΔ*vps*. The plasmid pKR6KΔ*vps* was transformed into strain *E. coli* S17-1. The derived *E. coli* S17-1 harboring pKR6KΔ*vps* plasmid was used as the donor in conjugation with strain Vmax. The conjugation and gene knockout with pKR6K plasmids was performed as below. First, incubate *E. coli* S17-1 harboring pKR6KΔ*vps* and Vmax to an OD_{600} of around 0.6. Then, mix the bacterial solution in a 5:1 ratio (donor bacteria: recipient bacteria) and centrifuge at 5000 r.p.m. for 10 min. The cell pellets were washed twice with saline solution (0.9%). After resuspension of the cells in a small amount of saline solution, they were dropped onto LB plates and incubated at 37°C overnight. Next, the bacteria colony on the plate was washed off with PBS buffer, collected in a centrifuge tube and centrifuged at 5000 r.p.m. for 10 min. The cell pellets were washed twice with PBS buffer. The bacterial suspensions were plated on MKO (20.0 g of glucose, 15.0 g of NaCl, 10.0 g of K_2HPO_4, 2.0 g of KH_2PO_4, 3.3 g of $(NH_4)_2SO_4$, 0.1 g of $MgSO_4{\cdot}7H_2O$, 5.0 g of $CaCO_3$, 3.2 mg of $CaCl_2{\cdot}2H_2O$, 3.8 mg of $ZnCl_2$, 0.03 g of $FeCl_3{\cdot}6H_2O$, 11.1 mg of $MnCl_2{\cdot}4H_2O$, 0.96 mg of $CuCl_2{\cdot}2H_2O$, 2.6 mg of $CoCl_2{\cdot}6H_2O$, 0.35 mg of H_3BO_3, 0.024 mg of $Na_2MoO_4{\cdot}2H_2O$ per liter) agar plates with chloramphenicol and kanamycin resistance to screen out correct recombinant strains. Then pass the correct recombinant strains for 2 generations in LBv2 medium. After diluting the bacterial solution to 10^{-5}, the bacterial solution was plated onto LBS (supplementing 150.0 g l^{-1} sucrose based on LBv2 medium) agar plates at 37°C overnight. The single colonies were plated on the LBv2 agar plates with and without chloramphenicol resistance at the same time to screen out the correct gene knockout strains. Finally, select the correct mutant strains further by PCR verification. The correct mutant strain was stored in glycerine at −80°C until use.

Biosynthesis of L-DOPA by a two-stage fed-batch strategy

After the cells were cultured, induced, collected, and washed as described above, cell pellets were suspended and stored at −80°C until use. The biosynthesis of L-DOPA was conducted in a 1-l stirred bioreactor with substrates fed at regular intervals. The initial reaction mixture contained phosphate buffer solution, 7.5 g l^{-1} of catechol, 10.0 g l^{-1} of pyruvate sodium, 50.0 g l^{-1} of ammonium acetate, 2.0 g l^{-1} of sodium sulfite, 1.0 g l^{-1} of ethylenediamine tetraacetic acid disodium salt, 1 mM of PLP, and resting cells of Vmax-1 or Vmax-2 or BL21-1 with a final OD_{600} of 20. And the reaction was conducted at 20°C and the pH was fixed at 8.0 adjusted by ammonia. In the first 4 h, 7.0 g l^{-1} of catechol, 7.0 g l^{-1} of pyruvate sodium, 5.6 g l^{-1} of ammonium acetate were fed every hour to maintain a constant concentration of substrates. With the proceeding of this process, the catalytic activities decreased. Accordingly, the feeding strategy was regulated to supply 3.5 g l^{-1} of catechol, 3.5 g l^{-1} of pyruvate sodium, and 2.8 g l^{-1} of ammonium acetate every hour for the rest of the whole-cell catalysis process. Samples were taken every hour and further analyzed by HPLC to detect the concentrations of catechol and L-DOPA.

Analytic methods

All samples were dissolved in the same volume of 4 M HCl and centrifuged at 10 000 *g* for 5 min, which was diluted to appropriate multiples before analysis. Then samples were filtrated to remove the impurities. Samples were further analyzed and separated by C18 column (Welch, 250 × 4.6 mm) of HPLC system (Agilent, 1260 Infinity II) equipped with a UV detector (Diode-Array Detector, DAD). The mobile phase consists of 90% 20 of mM KH_2PO_4 (pH 2.6) and 10% methanol at a flow rate of 1 ml min^{-1}. The column temperature was maintained at 30°C and the injection volume was set as 10 μl. The analysis was performed at a wavelength of 280 nm.

Acknowledgements

This study was supported by the grant of the National Key R&D Program of China (2017YFC1600100).

Conflict of interest

None declared.

References

Becker, W., Wimberger, F., and Zangger, K. (2019) *Vibrio natriegens*: An alternative expression system for the high-yield production of isotopically labeled proteins. *Biochemistry* **58:** 2799–2803.

Chandel, M., and Azmi, W. (2013) Purification and characterization of tyrosine phenol lyase from *citrobacter freundii*. *Appl Biochem Biotechnol* **171:** 2040–2052.

Chattopadhyay, S., Datta, S.K., and Mahato, S.B. (1994) Production of L-DOPA from cell suspension culture of *Mucuna pruriens f.* pruriens. *Plant Cell Rep* **13:** 519–522.

Das, A., Tyagi, N., Verma, A., Akhtar, S., and Mukherjee, K.J. (2018) Metabolic engineering of *Escherichia coli* W3110 strain by incorporating genome-level modifications and synthetic plasmid modules to enhance L-DOPA production from glycerol. *Prep Biochem Biotechnol* **48:** 671–682.

Demidkina, T.V., Anston, A.A., Faleev, N.G., Phillips, R.S., and Zakomyrdina, L.N. (2009) Spatial structure and mechanism of tyrosine phenol-lyase and tryptophan indole-lyase. *Mol Biol (Mosk)* **43:** 295–308.

Dorsey, E.R., Sherer, T., Okun, M.S., and Bloem, B.R. (2018) The emerging evidence of the Parkinson pandemic. *J Parkinsons Dis* **8:** S3–S8.

Eagon, R.G. (1962) *Pseudomonas natriegens*, a marine bacterium with a generation time of less than 10 minutes. *J Bacteriol* **83:** 736–737.

Enei, H., Nakazawa, H., Okumura, S., and Yamada, H. (1973) Synthesis of L-tyrosine or 3, 4-dihydroxyphenyl-L-alanine from pyruvic acid, ammonia and phenol or pyrocatechol. *Agric Biol Chem* **37:** 725–735. https://doi.org/10.1080/00021369.1973.10860755

Fagerbakke, K., Heldal, M., and Norland, S. (1996) Content of carbon, nitrogen, oxygen, sulfur and phosphorus in native aquatic and cultured bacteria. *Aquat Microb Ecol* **10:** 15–27.

Collaborators, G.B.D.N. (2019) Global, regional, and national burden of neurological disorders, 1990–2016: A systematic analysis for the global burden of disease study 2016. *Lancet Neurol* **18:** 459–480.

Fong, J.C.N., Syed, K.A., Klose, K.E., and Yildiz, F.H. (2010) Role of *Vibrio* polysaccharide (*vps*) genes in VPS production, biofilm formation and *Vibrio cholerae* pathogenesis. *Microbiology (Reading)* **156:** 2757–2769.

Han, H., Xu, B., Zeng, W., and Zhou, J. (2020) Regulating the biosynthesis of pyridoxal 5′-phosphate with riboswitch to enhance L-DOPA production by *Escherichia coli* whole-cell biotransformation. *J Biotechnol* **321:** 68–77.

Hoff, J., Daniel, B., Stukenberg, D., Thuronyi, B.W., Waldminghaus, T., and Fritz, G. (2020) *Vibrio natriegens*: An ultrafast-growing marine bacterium as emerging synthetic biology chassis. *Environ Microbiol* **22:** 4394–4408.

Hoffart, E., Grenz, S., Lange, J., Nitschel, R., Müller, F., Schwentner, A., *et al.* (2017) High substrate uptake rates empower *Vibrio natriegens* as production host for industrial biotechnology. *Appl Environ Microbiol* **83:** e01614–e1617.

Katayama, T., and Kumagai, H. (2010) *L-DOPA, microbial production*. Hoboken, NJ: Wiley. https://doi.org/10.1002/9780470054581.eib258

Koyanagi, T., Katayama, T., Suzuki, H., Nakazawa, H., Yokozeki, K., and Kumagai, H. (2005) Effective production of 3,4-dihydroxyphenyl-L-alanine (L-DOPA) with *Erwinia herbicola* cells carrying a mutant transcriptional regulator TyrR. *J Biotechnol* **115:** 303–306.

Krishnaveni, R., Rathod, V., Thakur, M.S., and Neelgund, Y.F. (2009) Transformation of L-tyrosine to L-DOPA by a novel fungus, *Acremonium rutilum*, under submerged fermentation. *Curr Microbiol* **58:** 122–128.

Kumagai, H., Yamada, H., Matsui, H., Ohkishi, H., and Ogata, K. (1970) Tyrosine phenol lyase. I. Purification, crystallization, and properties. *J Biol Chem* **245:** 1767–1772.

Lee, J.Y., and Xun, L.Y. (1998) Novel biological process for L-DOPA production from L-tyrosine by *p*-hydroxyphenylacetate 3-hydroxylase. *Biotechnol Lett* **20:** 479–482.

Lee, S.G., Ro, H.S., Hong, S.P., Kim, E.H., and Sung, M.H. (1996) Production of L-dopa by thermostable tyrosine phenol-lyase of a thermophilic *Symbiobacterium species* overexpressed in recombinant *Escherichia coli*. *J Microbiol Biotechnol* **6:** 98–102.

Lin, B., and Tao, Y. (2017) Whole-cell biocatalysts by design. *Microb Cell Fact* **16:** 106.

Milic, D., Demidkina, T.V., Faleev, N.G., Phillips, R.S., Matkovic-Calogovic, D., and Antson, A.A. (2011) Crystallographic snapshots of tyrosine phenol-lyase show that substrate strain plays a role in c-c bond cleavage. *J Am Chem Soc* **133:** 16468–16476.

Min, K., Kathavarayan, T., Park, K., and Yoo, Y.J. (2013) Novel strategy for enhancing productivity in L-DOPA synthesis: The electroenzymatic approach using well-dispersed L-tyrosine. *J Mol Catal B-Enzym* **90:** 87–90. https://doi.org/10.1016/j.molcatb.2013.01.027

Min, K., Park, K., Park, D.H., and Yoo, Y.J. (2015) Overview on the biotechnological production of L-DOPA. *Appl Microbiol Biotechnol* **99:** 575–584.

Nagatsua, T., and Sawadab, M. (2009) L-DOPA therapy for Parkinson's disease: Past, present, and future. *Parkinsonism Relat Disord* **15:** S3–8.

Park, H.S., Lee, J.Y., and Kim, H.S. (1998) Production of L-dopa(3,4-dihydroxyphenyl-L-alanine) from benzene by using a hybrid pathway. *Biotechnol Bioeng* **58:** 339–343.

Sayyed, I.A., and Sudalai, A. (2004) Asymmetric synthesis of L-DOPA and (*R*)-selegiline via, OsO_4-catalyzed asymmetric dihydroxylation. *Tetrahedron-Asymmetry* **15:** 3111–3116. https://doi.org/10.1016/j.tetasy.2004.08.007

Schwechheimer, C., Hebert, K., Tripathi, S., Singh, P.K., Floyd, K.A., Brown, E.R., *et al.* (2020) A tyrosine phosphoregulatory system controls exopolysaccharide biosynthesis and biofilm formation in *Vibrio cholerae*. *PLoS Pathog* **16:** e1008745.

Tang, X.L., Liu, X., Suo, H., Wang, Z.C., Zheng, R.C., and Zheng, Y.G. (2018) Process development for efficient biosynthesis of L-DOPA with recombinant *Escherichia coli* harboring tyrosine phenol lyase from *Fusobacterium nucleatum*. *Bioprocess Biosyst Eng* **41:** 1347–1354.

Trunk, T., Khalil, H.S., and Leo, J.C. (2018) Bacterial autoaggregation. *AIMS Microbiol* **4:** 140–164.

Tschirhart, T., Shukla, V., Kelly, E.E., Schultzhaus, Z., Newringeisen, E., Erickson, J.S., *et al.* (2019) Synthetic

biology tools for the fast-growing marine bacterium *Vibrio natriegens*. *ACS Synth Biol* **8:** 2069–2079.

Valdés, R.H., Puzer, L., Gomes, M., Marques, C.E.S.J., Aranda, D.A.G., Bastos, M.L., *et al*. (2004) Production of L-DOPA under heterogeneous asymmetric catalysis. *Catal Commun* **5:** 631–634. https://doi.org/10.1016/j.catcom.2004.07.018

Weinstock, M.T., Hesek, E.D., Wilson, C.M., and Gibson, D.G. (2016) *Vibrio natriegens* as a fast-growing host for molecular biology. *Nat Methods* **13:** 849–+.

Xu, J.Q., Dong, F., Wu, M.X., Tao, R.S., Yang, J.J., Wu, M.B., *et al*. (2021) *Vibrio natriegens* as a pET-compatible expression host complementary to *Escherichia coli*. *Front Microbiol* **12:** 627181.

Yuan, W., Zhong, S., Xiao, Y., Wang, Z., and Sun, J. (2020) Efficient biocatalyst of L-DOPA with *Escherichia coli* expressing a tyrosine phenol-lyase mutant from *Kluyvera intermedia*. *Appl Biochem Biotechnol* **190:** 1187–1200.

Zeng, W.Z., Xu, B.B., Du, G.C., Chen, J., and Zhou, J.W. (2019) Integrating enzyme evolution and high-throughput screening for efficient biosynthesis of L-DOPA. *J Ind Microbiol Biotechnol* **46:** 1631–1641.

Zhang, Y., Li, Z., Liu, Y., Cen, X., Liu, D., and Chen, Z. (2021) Systems metabolic engineering of *Vibrio natriegens* for the production of 1,3-propanediol. *Metab Eng* **65:** 52–65.

Zheng, R.C., Tang, X.L., Suo, H., Feng, L.L., Liu, X., Yang, J., and Zheng, Y.G. (2018) Biochemical characterization of a novel tyrosine phenol-lyase from *Fusobacterium nucleatum* for highly efficient biosynthesis of L-DOPA. *Enzyme Microb Technol* **112:** 88–93.

Zhu, H.Q., Tang, X.L., Zheng, R.C., and Zheng, Y.G. (2020) Purification and biochemical characterization of a tyrosine phenol-lyase from *Morganella morganii*. *Appl Biochem Biotechnol* **192:** 71–84.

Supporting information

Additional supporting information may be found online in the Supporting Information section at the end of the article.

Fig S1. SDS-PAGE analysis of the effect of induction time on protein expression at 37°C by *V. natriegens*. The numbers correspond to the time of induction.

Fig S2. Optimization of protein expression at 16°C by *E.coli* over induction time. (A) SDS-PAGE analysis of the effect of induction time on protein expression. From left to right, the induction time was 0, 4, 8, 12, 16, 20h, respectively. The left half represented supernatants and the right half represented precipitates. (B) The curve of relative quantitative of soluble protein expression over induction time. Red square represented OD_{600} and black circle represented relative protein expression.

Fig S3. Phenomenon of bacterial autoaggregation. (A) Top view of the bioreactor. (B) Lateral view of the bioreactor.

Table S1. Bacterial strains used in this study.

